Cost-Effective Energy Management of a Microgrid Using a Hybrid Yellow Saddle Goatfish Optimization Algorithm

Asadullah Younas[1*], Tahir Mahmood[1], Muhammad Mansoor Ashraf[1]
[1]Department of Electrical Engineering, University of Engineering and Technology Taxila, Pakistan
***Correspondence**: asadullahyounas1020@gmail.com

Citation | Younas. A, Mahmood. T, Ashraf. M. M, "Cost-Effective Energy Management of a Microgrid Using a Hybrid Yellow Saddle Goatfish Optimization Algorithm", IJIST, Vol. 07 Special Issue pp 158-171, May 2025
Received | April 07, 2025 **Revised |** May 10, 2025 **Accepted |** May 11, 2025 **Published |** May 12, 2025.

The increasing integration of renewable energy sources into hybrid Microgrid presents challenges such as power fluctuations, system complexity, and high operational costs. This paper proposes an optimized energy management framework that combines the Hybrid Yellow Saddle Goatfish Optimization Algorithm (HYSGA) with Sequential Quadratic Programming (SQP) to improve system efficiency, stability, and cost-effectiveness. The HYSGA approach efficiently manages energy distribution among solar photovoltaic (PV) systems, Battery Energy Storage Systems (BESS), and the power grid, ensuring reliable and cost-effective operation. HYSGA quickly identifies near-optimal solutions for complex energy management issues, while SQP fine-tunes these solutions to improve precision and convergence speed. Extensive simulations and cost comparisons confirm the framework's performance. In the baseline scenario, the hybrid Microgrid incurs an annual operational cost of $26,900. In Case I, this cost drops to $13,800, achieving 49% savings. Further optimization with HYSGA reduces the cost to $13,430.08, resulting in a 50.118% savings. Additionally, comparative evaluations show that HYSGA outperforms traditional techniques like Mixed-Integer Nonlinear Programming (MINLP) in terms of cost savings, computational efficiency, and solution accuracy. This study provides a detailed analysis of the research methodology, solution approach, and performance evaluation, ensuring clarity. The results demonstrate that the HYSGA framework is a scalable, computationally efficient, and economically viable solution for hybrid Microgrid energy management. The proposed method offers a promising approach for enhancing energy efficiency and reducing costs in modern smart grid applications.

Keywords: Microgrid, Energy Management, PV, BESS, HYSGA, SQP

Introduction:

A Microgrid is a local power network that combines power-consuming devices and small-scale energy sources. It operates independently, responding quickly to grid demands, and can be tailored to meet specific user needs. Benefits of Microgrid include improved reliability, reduced feeder losses, voltage support, efficient use of waste heat, voltage sag correction, and uninterrupted power supply [1]. The U.S. Department of Energy defines Microgrid as networks of connected loads and distributed energy resources (DERs) with clear electrical boundaries. A Microgrid operates under a single control unit, demonstrating the ability to function both on and off the grid [2]. With rising power demand, the need for renewable energy sources grows to ensure energy expansion and sustainability. Microgrid support decentralized energy management, facilitating efficient coordination between consumers and generation units. By integrating local energy resources, they improve resilience and support the transition to greener energy [3]. Microgrid control systems help manage energy distribution, ensuring power is supplied at minimal operational costs [4].

Various control methods are used to optimize Microgrid performance by enabling intelligent management of energy resources and power loads [5]. However, sub-optimal Microgrid energy management under unpredictable conditions remains a challenge for techniques like mixed-integer linear programming, linear programming, and dynamic programming. These methods struggle with high-dimensional systems and are not adaptable to changes like fluctuating load demands and renewable energy patterns [6], [7]. To address this, metaheuristic techniques such as Particle Swarm Optimization (PSO) and Genetic Algorithms (GA) are often combined. However, these methods have long processing times, making them unsuitable for real-time applications, and they lack the ability to retain knowledge for future tasks, reducing their computational efficiency over time [8], [9]. Furthermore, their performance is compromised without accurate models and proper forecasting methods. Metaheuristic techniques are often combined with linear techniques to leverage their complementary strengths [10].

Energy management in Microgrid involves advanced optimization techniques like linear, non-linear, Mixed-integer, and robust programming. Common metaheuristic algorithms include PSO, GA, Artificial Bee Colony, and Bacterial Foraging. Additionally, intelligent methods such as Fuzzy Logic and Evolutionary Algorithms enhance performance, while approaches like Dynamic Programming, Game Theory, Model Predictive Control, and Multi-Agent Systems help improve decision-making for effective energy resource management [11]. Microgrid integrate distributed generators and loads to operate as a single controllable unit, but managing hybrid Microgrid is complex due to renewable variability and cost-efficiency demands. This article addresses hybrid Microgrid energy management by combining Hybrid Yellow Saddle Goatfish Optimization with Sequential Quadratic Programming (HYSGA-SQP). This method optimizes decision variables, reducing the total operating cost of the Microgrid [12]. The article follows a structured format, with Section III presenting the mathematical modeling of the problem, Section IV explaining the HYSGA-SQP algorithm, Section V showing simulation results, and Section VI concluding the study. Section VII provides acknowledgements.

Objectives:

This study focuses on implement Cost-Effective Energy Management of a Microgrid Using a Hybrid Yellow Saddle Goatfish Optimization Algorithm. A Hybrid Yellow Saddle Goatfish Optimization Algorithm is proposed to address the Cost-Effective Energy Management of a Microgrid problem. Objectives of the Study are:

1. To implement the YSGFA algorithm tailored for cost-effective energy management in a hybrid microgrid.

2. To integrate the developed YSGFA algorithm with SQP for enhanced optimization of energy management in microgrid systems.

3. To evaluate the performance of the proposed algorithm through simulation studies and compare its effectiveness against existing optimization techniques.

Novelty Statement:

This study introduces a novel hybrid optimization framework combining the Hybrid Yellow Saddle Goatfish Optimization Algorithm (HYSGA) with Sequential Quadratic Programming (SQP) for efficient energy management in hybrid microgrids. Unlike conventional methods, the proposed HYSGA-SQP approach leverages the global search capabilities of HYSGA and the refinement accuracy of SQP to achieve superior performance in cost reduction, convergence speed, and operational reliability. The integration of these two algorithms presents a new, scalable solution that outperforms traditional techniques such as Mixed-Integer Nonlinear Programming (MINLP), demonstrating enhanced computational efficiency in 25 runs and 50.1180% cost savings in real-world microgrid scenarios.

Problem Formulation:

Objective Function:

Cost minimization for residential Microgrid involves two key cost components: $C_{grid}(\tau)$ and $C_{bat}(\tau)$, which are mathematically defined as an optimization problem in this study [12]. The primary goal is to minimize system costs related to energy consumption at various nodes across different time periods. The mathematical representation of this formula is shown below:

$$\mathrm{f(x)} = min \sum_{\tau=1}^{\tau=24} \left[C_{grid}(\tau) + C_{bat}(\tau)\right] \quad (1)$$

The operational cost optimization model outlined in equation (1) calculates the total expenses for both battery storage and grid power over a 24-hour period. Equations (2) to (6) estimate the battery costs while accounting for factors such as the battery's depth of discharge and charging state, as well as their impact on battery operation duration and grid system communication.

$$C_{bat}^{\tau} = -\left(C_{DOD} \Delta \wp(\tau) \Delta\tau\right) \quad (2)$$

$$C_{DOD} = C_{ici} \left| \frac{1}{L(DOD_2)} - \frac{1}{L(DOD_1)} \right| \Delta \wp(\tau) \Delta\tau \quad (3)$$

where, $\Delta \wp(\tau)$ is the battery power measured in kW and $\Delta\tau$ in hours.

$$\mathrm{DOD}(\tau) = 1 - \mathrm{SOC}(\tau) \quad (4)$$

$$C_{grid}(\tau) = -\left(G_{\tau}(\tau)\mathcal{P}_p(\tau).\Delta\tau - \upsilon G_{\tau}(\tau)\mathcal{P}_s(\tau).\Delta\tau\right) \quad (6)$$

The state space set (S) includes all possible system states at each time step τ, as shown in equation (7). The state variable $\mathfrak{s}_{\tau}$ in equation (8) represents the system's conditions at time τ, incorporating factors such as PV power output, SOC values, grid prices, and load requirements. Equation (9) defines the complete state space, covering all system states throughout the entire time period. Equation (10) calculates the net load demand by accounting for the power generated by the PV system and determining the remaining load requirements. The SOC management system, detailed in equations (11) and (12), controls battery energy delivery by calculating residual load needs and forecasting future SOC values, ensuring that SOC restrictions are respected [12].

$$\mathrm{S} = \{\mathrm{S}_{\tau}\} \quad (7)$$

$$\mathfrak{s}_{\tau} = \{\tau, \mathcal{P}_{\tau}^{PV}, \mathrm{SOC}_{\tau}, G_{\tau}, \mathcal{P}_{l,\tau}\} \quad (8)$$

$$\mathcal{S} = \mathfrak{s}_0 \cup \mathfrak{s}_1 \cup \mathfrak{s}_2 \cup \dots \dots \cup \mathfrak{s}_{T-1} \quad (9)$$

$$\mathcal{P}_{ld,\tau}^{NET} = max\left(\left(\mathcal{P}_{ld,\tau} - \mathcal{P}_{\tau}^{pv}\right), 0\right) \quad (10)$$

$$\mathcal{P}_{ld,\tau}^{REM} = max\left(\mathcal{P}_{ld,\tau}^{NET} - \left(SOC_{\tau} - SOC^{min}\right).E, 0\right) \quad (11)$$

$$SOC_{\tau}^{NEXT} = min\,(SOC^{max}, \left(max(\mathcal{P}_{\tau}^{pv} - \mathcal{P}_{ld,\tau}, 0) + max\left(\frac{(SOC_{\tau} - SOC^{min}).Ę - \mathcal{P}_{ld,\tau}^{NET}}{Ę}, 0\right)\right) \quad (12)$$

$$Action_{\mathfrak{s}_{\tau}} = \{-\mathcal{K}\Delta\wp, \ldots, -\Delta\wp, 0, \Delta\wp, \ldots, \mathcal{K}\Delta\wp\} \quad (13)$$

$$B_{ESS}(\mathcal{A}_{\tau}) = \{-\frac{\mathcal{K}(\mathcal{A}_{\tau})}{Ę}, \quad if\ \mathcal{A}_{\tau} = discharge \quad \frac{\mathcal{K}(\mathcal{A}_{\tau})}{Ę}, \quad \text{if } \mathcal{A}_{\tau} = \text{charge}\} \quad (14)$$

At each time step τ, the grid cost is updated through equation (15), which incorporates information about remaining load requirements and the functions of the battery energy storage system (BESS). Equation (16) adds the remaining load and BESS discharge into the cost calculation, factoring in the grid price multiplier. The battery cost, as calculated in equation (17), accounts for net load requirements and State of Charge (SOC) constraints to ensure alignment with grid pricing within the battery's operational boundaries. Equation (18) introduces the opportunity cost from SOC limit deviations, applying penalties for excessive charging or discharging. Finally, the reward function for states $\mathfrak{s}_{\tau}$ and actions $\mathcal{A}_{\tau}$ is determined in equation (19), encompassing all cost components.

$$C_{grid}^{\tau} = -(\mathcal{P}_{ld,\tau}^{REM} + B_{ESS}(\mathcal{A}_{\tau}).Ę).\,G_{\tau} \quad (15)$$

$$C_{p}^{\tau} = \mathcal{P}_{ld,\tau}^{REM} + B_{ESS}(a_{\tau.discharge}).Ę).\,G_{\tau}.\upsilon \quad (16)$$

$$C_{b}^{\tau} = \{\mathcal{P}_{ld,\tau}^{NET}.G_{\tau} \quad if\ \mathcal{P}_{ld,\tau}^{NET} \leq (SOC_{\tau} - SOC^{min}).Ę \quad \text{else } (SOC_{\tau} - SOC^{min}).\,G_{\tau}.\,Ę\} \quad (17)$$

$$C_{o}^{\tau} = \{-((SOC_{\tau} + \mathcal{K}(\mathcal{A}_{\tau}) - SOC^{max}).\,G_{\tau}.\,Ę \quad \text{if } (SOC_{\tau} + \mathcal{K}(\mathcal{A}_{\tau}) > SOC^{max} \quad -(|\mathcal{K}(\mathcal{A}_{\tau})| - (SOC_{\tau} + SOC^{max})).\,G_{\tau}.\,Ę \quad \text{else if } (SOC_{\tau} + \mathcal{K}(\mathcal{A}_{\tau}) < SOC^{min} \quad \text{else } 0\} \quad (18)$$

$$\mathcal{R}(\mathfrak{s}_{\tau}, \mathcal{A}_{\tau}) = C_{grid}^{\tau} + C_{bat}^{\tau} + C_{b}^{\tau} + C_{o}^{\tau} \quad (19)$$

Equation (20) defines the value function $\mathcal{V}_{\tau}^{\pi}(\mathfrak{s})$, which represents the cumulative reward starting from state $\mathfrak{s}_{\tau}$ and action $\mathcal{A}_{\tau}$, discounted over future time steps. This value function evaluates the long-term effectiveness of different strategies by summing immediate rewards and future discounted rewards. It helps guide the optimization process toward maximizing overall performance and cost efficiency [12].

$$\mathcal{V}_{\tau}^{\pi}(\mathfrak{s}) = \mathcal{R}(\mathfrak{s}_{\tau}, \mathcal{A}_{\tau}) + \sum_{i=1}^{\infty} \Upsilon^{i}.\mathcal{R}(\mathfrak{s}_{\tau+1}, \mathcal{A}_{\tau+1}) \quad (20)$$

Yellow Saddle goatfish optimization algorithm:

Zaldivar et al. [13] introduced the Yellow Saddle Goatfish Optimization Algorithm (YSGA) in 2018. The Yellow Saddle Goatfish displays a unique cooperative behavior, which is one of the most fascinating aspects of their collaborative hunting strategy. In this strategy, the fish are divided into smaller groups that evenly cover the entire exploitation area. Each sub-population works together in dual roles as Chasers and Blockers to carry out the hunt.

The YSGA mathematical model, developed by the authors, utilizes objective function variables C_{grid}^{τ} and C_{bat}^{τ} to effectively manage Microgrid costs.

First Phase: Exploration:

The goatfish population $\mathfrak{p}$ consists of x individuals $\{\mathfrak{p}_1, \mathfrak{p}_2, \mathfrak{p}_3 \ldots, \mathfrak{p}_x\}$, uniformly distributed within a y-dimensional search space defined by upper boundary $\mathcal{B}^{high}$ and lower boundary $\mathcal{B}^{low}$. Each individual $\mathfrak{p}_i$ is represented as a vector of decision variables $\{\mathfrak{p}_i^1, \mathfrak{p}_i^2, \mathfrak{p}_i^3 \ldots, \mathfrak{p}_i^x\}$. The initialization is defined by Equation (21).

$$\beta_i^j = rand.\left(B_j^{high} - B_j^{low}\right) + B_j^{low} \quad (21)$$
$$i = 1,2,\ldots,x; \quad j = 1,2,\ldots,y$$

Where $rand$ is a random number among [0,1].
Equation (22) calculates the squared error between μ_ℓ and the data points $\{\beta_1, \beta_2, \beta_3 \ldots, \beta_h\}$in cluster C_ℓ, using the goatfish population P as the data set.

$$e(C_\ell) = \sum_{\beta_g \in C_\ell} \| \beta_g - \mu_\ell \|^2 \quad (22)$$
$$g = 1,2,\ldots,h; \quad \ell = 1,2,\ldots,\kappa$$

The goal of k-means is to minimize the objective function, which represents the total sum of squared errors across all k clusters, as shown in Equation (23).

$$E(C) = \sum_{\ell=1}^{\kappa} e(C_\ell) \quad (23)$$

In a goatfish school, there is one chaser fish $\varphi_\ell \in \beta$, responsible for leading the pursuit, chosen based on its fitness value. Within each group, the particle with the highest fitness value is the closest to the solution, a behavior demonstrated through Lévy flight. This is a non-Gaussian random process that uses a Lévy stable distribution for random walks. The chaser fish uses random walks to change its position, aiming to find hidden prey in crevices. Equation (24) determines the new position of the chaser fish.

$$\varphi_\ell^{\tau+1} = \varphi_\ell^\tau + \alpha \oplus \text{Lévy}(\beta) \quad (24)$$
$$0 < \beta \leq 2$$

The chaser fish's new and current positions are represented by $\varphi_\ell^{\tau+1}$ and φ_ℓ^τ, respectively. α denotes the step size, $\oplus$ indicates element-wise multiplication, and β is the Lévy index, which controls the shape of the probability distribution, especially its tail. Equation (25) defines the value of β\betaβ.

$$\beta = 1.99 + \frac{0.001\tau}{\tau_{max}/10} \quad (25)$$

Typically, each group ignores other sub-populations and focuses solely on the group that captures the best prey. This behavior is expressed in Equation (26).

$$S = \alpha \oplus \text{Lévy}(\beta) \sim \alpha\left(\frac{u}{|v|^{1/\beta}}\right)\left(\varphi_\ell^\tau - \varphi_{best}^\tau\right) \quad (26)$$

In this scenario, S represents the random step, while φ_{best}^τ denotes the most successful chaser fish among all the clusters. Using Γ as the Gamma function, the parameters σ_u and σ_v are formulated in Equation (27).

$$\sigma_u = \left\{\frac{\Gamma(1+\beta)\sin\frac{\pi\beta}{2}}{\Gamma\left(\frac{1+\beta}{2}\right)\beta 2^{(\beta-1)/2}}\right\}^{1/\beta} \quad , \sigma_v = 1 \quad (27)$$

On behalf of given statements, the revised location of the chaser fish outlined in (24) can be updated in (28).

$$\varphi_\ell^{\tau+1} = \varphi_\ell^\tau + S \quad (28)$$

Consequently, the new position of the best chaser fish is computed using (29).

$$\varphi_{Best}^{\tau+1} = \varphi_{Best}^\tau + S' \quad (29)$$

Where, S' is formulated in (30)

$$S' = \alpha\left(\frac{u}{|v|^{1/\beta}}\right) \quad (30)$$

The strategy employed by blocker fish $\Phi_g \in \beta$ during hunting is to encircle the corals, cutting off escape routes for prey, while chaser fish attempt to capture the prey. The fish use a spiral algorithm to capture prey. Equation (31) calculates the new position of the blocker fish $\Phi_g^{\tau+1}$ based on the spiral algorithm.

$$\Phi_{g}^{\tau+1} = \mathcal{D}_{g} . e^{b\rho} . \cos 2\pi\rho + \varphi_{\ell} \quad (31)$$

In this context, the distance between the blocker and chaser fish along the spiral path is determined by the random number ϱ, which falls within the range of [$\boldsymbol{a}$, 1]. To enhance exploitation, $\boldsymbol{a}$ linearly decreases from -1 to -2 as the iteration count increases. The parameter $\mathfrak{b}$ is a fixed value that controls the form and orientation of the spiral; for this method, $\mathfrak{b}$ is set to 1. Equation (32) calculates the distance $\mathcal{D}_{g}$ between the current position of the blocker fish Φ_{g}^{τ} and the chaser fish in the cluster $\mathcal{C}_{\ell}$

$$\mathcal{D}_{g} = |r . \varphi_{\ell} - \Phi_{g}^{\tau}| \quad (32)$$

$$\{\varphi_{\ell} ,\ \Phi_{g}^{\tau}\} \in \mathcal{C}_{\ell}$$

Where r is a random number in the range of [-1, 1].

Once the hunting area is fully depleted, the group moves to a new location in search of more prey. The YSGA model includes an over-exploitation parameter (λ), if no better solution is found after λ iterations, the hunt is considered successful, prompting the goatfish in the cluster to relocate. This is described in Equation (33).

$$\beta_{g}^{\tau+1} = \frac{\varphi_{Best} + \beta_{g}^{\tau}}{2} \quad (33)$$

Methodology:

The proposed methodology integrates the Goat Fish Algorithm (GFA), a nature-inspired population-based optimization technique, with the deterministic Sequential Quadratic Programming (SQP) method to achieve a robust hybrid optimization framework. Initially, the algorithm begins by reading the test system data and initializing the Goat Fish population within the defined search space. During the exploration phase, the fitness of each individual is evaluated, and the population is partitioned into clusters consisting of Chaser Fish and Blocker Fish. These roles are dynamically updated based on relative fitness to encourage effective exploration and diversification. In the exploitation phase, promising solutions are refined by updating the global best fish and employing a counter-based mechanism to escape local optima when stagnation is detected. To further enhance convergence accuracy and fine-tune the best solution obtained from GFA, the method incorporates SQP, which approximates the objective function using a second-order Taylor expansion. This leads to the formulation and solution of a quadratic programming (QP) subproblem, followed by line search and Hessian matrix updates. The algorithm iteratively continues until the maximum number of iterations is reached, at which point the global best solution is reported. Figure 1 illustrates an optimization framework for a Microgrid test system, combining the Yellow Saddle Goatfish Optimization Algorithm (YSGA) with Sequential Quadratic Programming (SQP) [14]. It depicts both exploration and exploitation phases to enhance energy management, optimize power distribution, and improve system efficiency. This hybrid approach ensures optimal decision-making for reliable Microgrid operations.

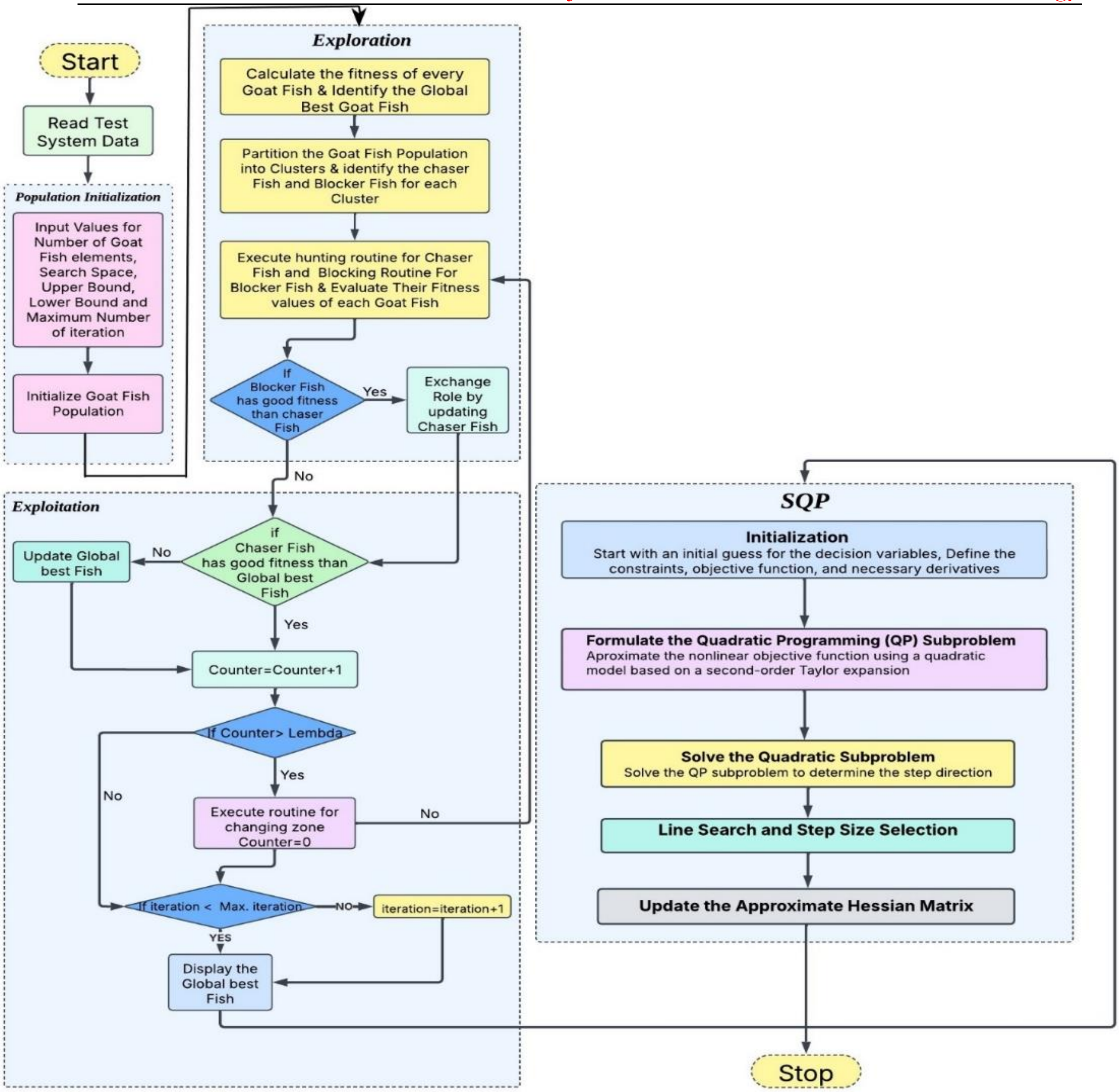

Figure 1. Flow Chart of HYSGA with SQP

Table I defines the decision variables and constants used in the optimization process for the cost-effective energy management of Microgrid.

Table 1. Optimal Decision Variable Values for HYSGA

Parameter	Value
C^{τ}_{total}	13430.08 $/Year
Cost Saving	50.118%
E_{BESS}	12 KWh
C^{τ}_{bat}	$2280
η_c, η_d	89%
DOD(τ)	20% - 80%
Battery Lifetime	7 Years
C^{τ}_{grid}	13430.08 $/Year
Payback Period	2 Months

ROI	589%
T	24Hours/day
Δt	1 Hour
SOC_{τ}	20% - 90%
$\mathcal{P}_{\tau}^{PV}$	5 KW
$\mathcal{P}_{l,\tau}$	40 KW
$\mathcal{P}_{ld,\tau}^{NET}$	15 - 30 KWh
$\mathcal{P}_{ld,\tau}^{REM}$	5 - 15 KWh
Γ_{τ}	\$0.07 -\$0.22/KWh
υ	10.8%
CSC	\$7.55/Month

Results:

This section evaluates the cost-effective energy management of a Hybrid Microgrid by combining the Hybrid Yellow Saddle Goatfish Optimization Algorithm (HYSGA) with Sequential Quadratic Programming (SQP) to assess its performance in energy management tasks. The total operating cost of the Microgrid is minimized by optimizing the decision variables $C_{grid}(\tau)$ and $C_{grid}(\tau)$. The effectiveness of HYSGA-SQP is also compared with other established optimization algorithms, highlighting its reliability in solving optimization challenges.

Figure 2 shows a hybrid Microgrid consisting of a Power Grid, PV array, BESS, and Load. It demonstrates efficient power flow between these components. The PV array powers the Load and charges the BESS. The BESS stores excess energy and supplies it when needed. The Grid supports the Load and BESS during periods of low solar output. This setup ensures continuous and reliable power delivery, with bidirectional flow between the BESS and the grid offering added flexibility. The system enhances efficiency and supports the integration of renewable energy.

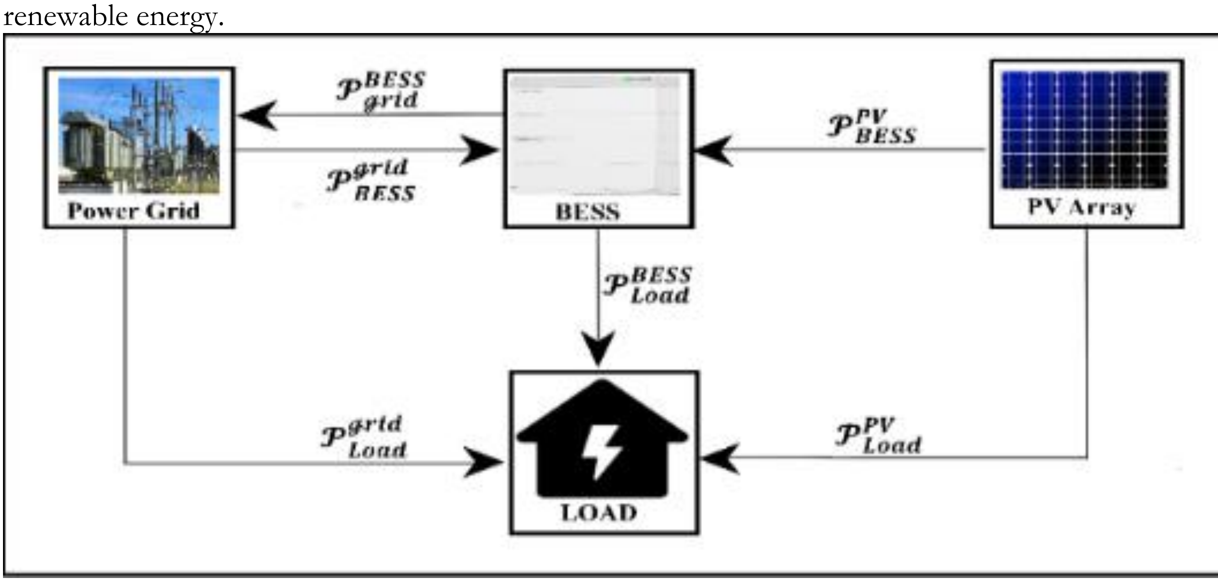

Figure 2. Microgrid Test System

Figures 3a and 3b highlight important aspects of cost-effective energy management in hybrid Microgrid. Figure 3a shows that as energy costs increase, savings decrease, emphasizing the importance of using low-cost renewables like solar and wind, along with efficient energy storage, to improve flexibility. Figure 3b illustrates a significant reduction in computational time with each optimization iteration, demonstrating improved algorithm efficiency and faster convergence for real-time decision-making. Together, these figures underline the need to lower costs and enhance computational performance for the sustainable operation of hybrid Microgrid.

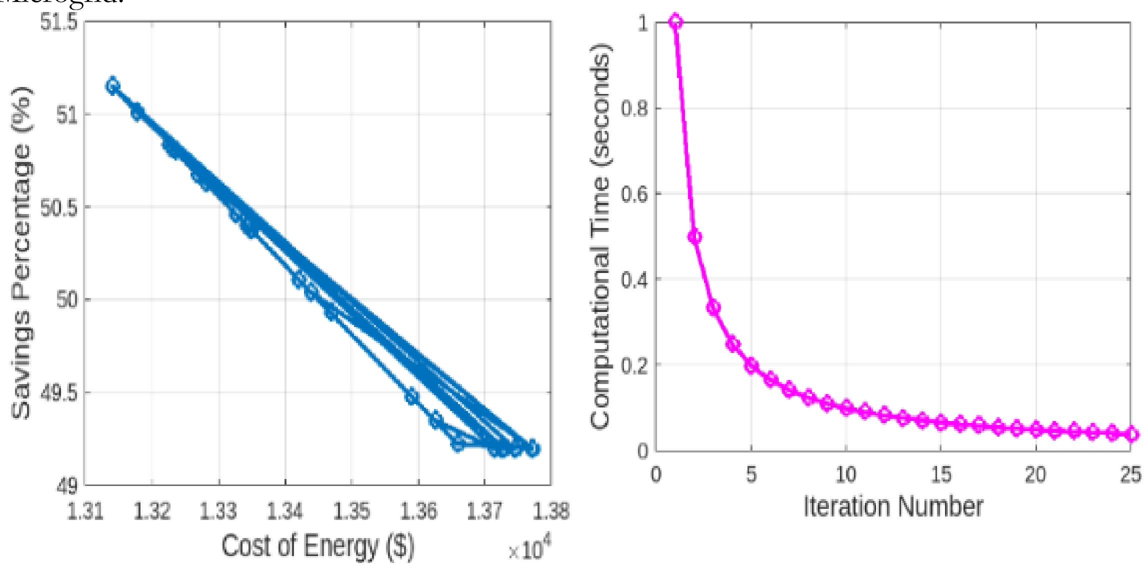

(a) (b)

Figure 3. (a) Cost of Energy vs Savings Percentage (b) Iteration Number vs Computational Time

Figure 4 shows the relationship between energy costs and savings percentage across multiple optimization iterations in hybrid Microgrid management. The blue curve represents energy costs, while the red curve shows savings. Their fluctuations highlight the algorithm's efforts to balance cost minimization with savings maximization, showcasing the challenge of finding equilibrium. This dynamic behavior emphasizes the need for adaptive energy dispatch strategies that account for load demand and renewable energy availability. Overall, the figure demonstrates improved responsiveness and performance in hybrid Microgrid operations.

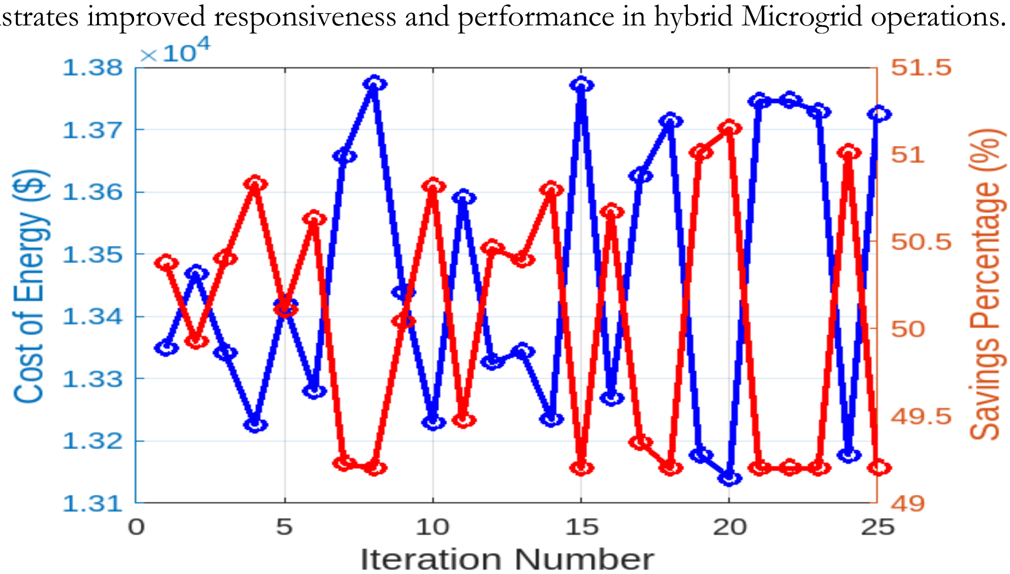

Figure 4. Iteration Number vs Cost of Energy and Savings Percentage

Figure 5 illustrates the savings percentage during hybrid Microgrid optimization, ranging from 49% to 51.5%. These fluctuations reflect the algorithm's adaptive approach in searching for cost-effective solutions, a characteristic of heuristic methods that use iterative energy dispatch adjustments. Despite the small oscillations, the overall high savings suggest a strong energy management strategy. The results highlight the trade-offs in cost optimization while maintaining system stability and demonstrate the system’s responsiveness to changing load and energy availability. Ultimately, the process aims for reliable and economical operation.

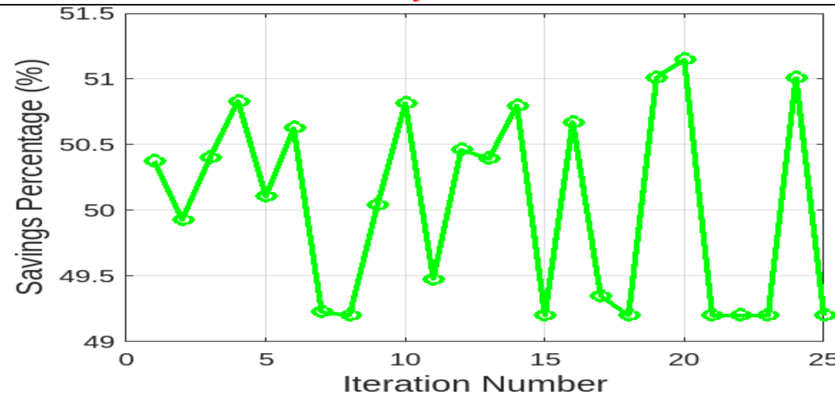

Figure 5. Iteration Number vs Savings Percentage

Figure 6 displays the baseline load profile of a hybrid Microgrid over 34 hours, highlighting fluctuations in daily demand. These peaks and valleys are essential for effective demand-side management. During high-demand periods, using storage or renewable energy sources can reduce reliance on the grid, while low-demand times are ideal for charging batteries or shifting loads. Understanding these patterns aids in forecasting and planning, aligning energy use with demand to enhance cost-efficiency and reliability.

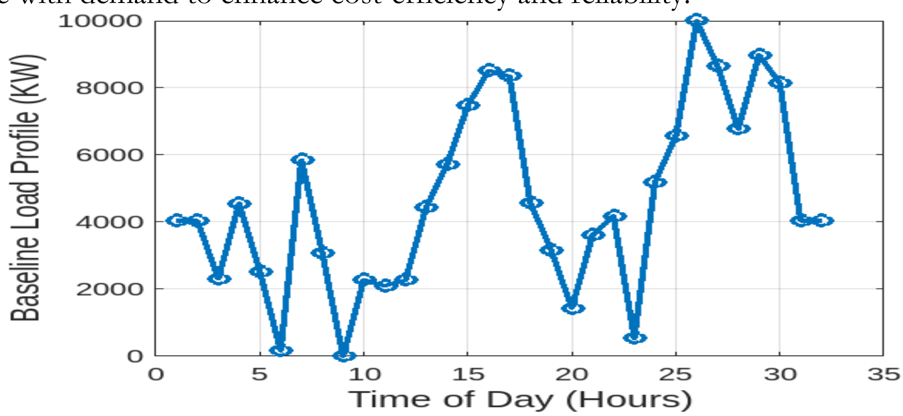

Figure 6. Baseline Load Profile vs Time of Day

Figure 7 shows variations in power output within a hybrid Microgrid, highlighting dynamic energy usage. A dip near zero between the 15th and 20th points suggests load shedding or reliance on stored energy. These fluctuations guide decisions to minimize generation or switch to more cost-effective sources. Analyzing these trends aids in cost-effective energy planning, optimizing the use of renewables and battery storage to ensure availability and reduce costs.

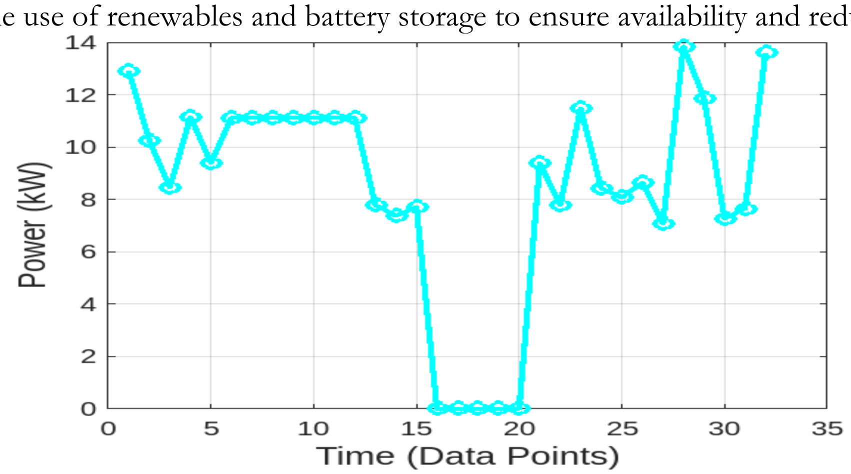

Figure 7. Power vs Time (32 Data Points)

Figure 8 shows the fitness values from different optimization runs for hybrid Microgrid energy management, highlighting performance variability. Higher fitness values indicate more effective energy strategies; run 7 achieves the highest value (13514.6), while run 16 shows the lowest (13358.0), reflecting less efficiency. This variation underscores the algorithm's stochastic nature. Multiple simulations foster convergence toward optimal solutions, enhancing decision-making for cost savings and system performance, emphasizing the importance of robust optimization in hybrid Microgrid management.

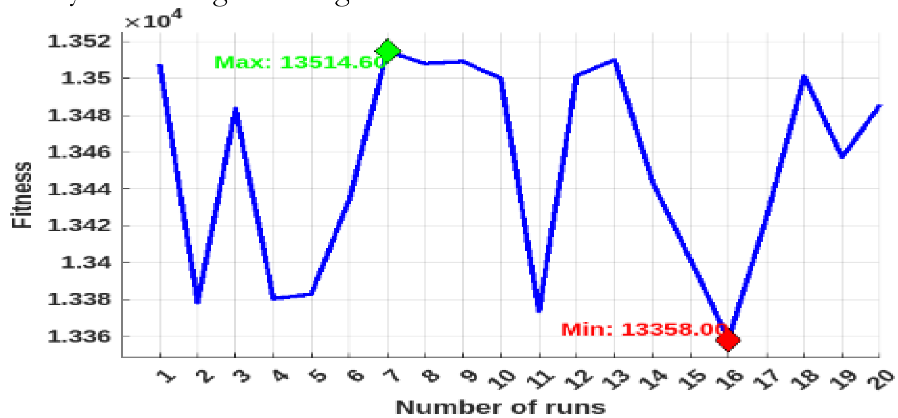

Figure 8. Fitness Value Vs Number of Runs

Discussion:

This section interprets the results, comparing HYSGA-SQP's effectiveness against existing optimization methods. Table II shows that HYSGA-SQP outperforms YSGA, reducing costs from $13,800 to $13,430.08 and increasing savings from 49 percent to 50.118 percent. Table III provides a run-wise comparison, confirming the algorithm's consistent performance with slight fluctuations due to its heuristic nature. Results affirm that integrating renewable sources, efficient storage, and intelligent optimization enhances microgrid sustainability, reducing reliance on high-cost grid power. HYSGA-SQP achieves faster convergence rates, ensuring quicker responses to real-time energy fluctuations, which is essential for practical applications requiring rapid optimization.

Table 2. Annual Energy cost and cost savings associated with baseline, Case 1, YSGA algorithm, and proposed Hysgs with SQP.

Parameter	Energy Cost ($/Year)	Cost Savings (%)
Baseline	26900 [10]	-
CASE 1	13800 [15]	49% [15]
YSGA	13447.16	50.06%
Proposed HYSGA with SQP	**13430.08**	**50.118%**

Table 3. Run-Wise Cost to Savings Comparison for Baseline and Case I for [15] vs Proposed HYSGA with SQP

Run No	Parameter	Baseline	CASE 1	HYSGA with SQP
1	Energy Cost ($/Year)	26900	13800	13429.16
	Cost Savings (%)	-	49%	50.12%
2	Energy Cost ($/Year)	26900	13800	13434.32
	Cost Savings (%)	-	49%	50.10%
3	Energy Cost ($/Year)	26900	13800	13438.12
	Cost Savings (%)	-	49%	50.09%
4	Energy Cost ($/Year)	26900	13800	13385.76
	Cost Savings (%)	-	49%	50.25%
5	Energy Cost ($/Year)	26900	13800	13479.0
	Cost Savings (%)	-	49%	49.99%
6	Energy Cost ($/Year)	26900	13800	13422.12
	Cost Savings (%)	-	49%	50.16%

Run No	Parameter	Baseline	CASE 1	HYSGA with SQP
7	Energy Cost ($/Year)	26900	13800	13437.28
	Cost Savings (%)	-	49%	50.07%
8	Energy Cost ($/Year)	26900	13800	13473.96
	Cost Savings (%)	-	49%	49.95%
9	Energy Cost ($/Year)	26900	13800	13416.92
	Cost Savings (%)	-	49%	50.15%
10	Energy Cost ($/Year)	26900	13800	13412.32
	Cost Savings (%)	-	49%	50.18%
11	Energy Cost ($/Year)	26900	13800	13451.60
	Cost Savings (%)	-	49%	50.04%
12	Energy Cost ($/Year)	26900	13800	13412.72
	Cost Savings (%)	-	49%	50.19%
13	Energy Cost ($/Year)	26900	13800	13360.04
	Cost Savings (%)	-	49%	50.36%
14	Energy Cost ($/Year)	26900	13800	13426.12
	Cost Savings (%)	-	49%	50.11%
15	Energy Cost ($/Year)	26900	13800	13375.52
	Cost Savings (%)	-	49%	50.29%
16	Energy Cost ($/Year)	26900	13800	13438.68
	Cost Savings (%)	-	49%	50.09%
17	Energy Cost ($/Year)	26900	13800	13467.88
	Cost Savings (%)	-	49%	49.99%
18	Energy Cost ($/Year)	26900	13800	13495.20
	Cost Savings (%)	-	49%	49.91%
19	Energy Cost ($/Year)	26900	13800	13425.16
	Cost Savings (%)	-	49%	50.15%
20	Energy Cost ($/Year)	26900	13800	13472.12
	Cost Savings (%)	-	49%	49.94%

Table 2 compares energy management strategies for a Microgrid, showing that the baseline scenario incurs a cost of $26,900, while Case I reduces this to $13,800, achieving 49% savings, the proposed Hybrid Yellow Saddle Goatfish Optimization Algorithm (HYSGA) with Sequential Quadratic Programming (SQP) yields the best optimal results, decreasing energy costs to $13,430.08 and maximizing savings at 50.118%.. Table III highlights the cost-to-savings ratios over 25 iterations, with the HYSGA using SQP performing the best, lowering costs to $13,430.08 and achieving maximum savings of 50.118%. These results confirm the algorithm's effectiveness and establish HYSGA with SQP as the optimal strategy.

Conclusion:

The proposed research presents a cost-effective energy management system (EMS) for hybrid Microgrid, using the Hybrid Yellow Saddle Goatfish Optimization Algorithm (HYSGA) combined with Sequential Quadratic Programming (SQP). This system optimizes energy scheduling under stochastic conditions, taking into account battery degradation costs and Time of Use (ToU) grid tariffs in a unified cost function. The performance of HYSGA with SQP is compared to the baseline scenario, where the grid is the sole energy supplier. In the baseline case, relying entirely on grid power incurs an annual energy cost of $26,900. The Microgrid retrofit in Case I reduces the energy cost to $13,800, achieving 49% savings. The proposed HYSGA with SQP algorithm further reduces the energy cost to $13,430.08, resulting in 50.118% savings. These results demonstrate that the HYSGA with SQP algorithm significantly enhances cost-effectiveness in the management of Microgrid energy systems.

Acknowledgment:

The authors hereby confirm that the manuscript has not been published previously, nor is it under consideration for publication elsewhere. All authors contributed equally to the research and preparation of this manuscript and are in full agreement with its content.

References:

[1] F. J. Wisam Kareem Meteab, Salwan Ali Habeeb Alsultani, "Energy Management of Microgrids with a Smart Charging Strategy for Electric Vehicles Using an Improved RUN Optimizer," *Energies*, vol. 16, no. 16, p. 6038, 2023, doi: https://doi.org/10.3390/en16166038.

[2] C. Guo, X. Wang, Y. Zheng, and F. Zhang, "Real-time optimal energy management of microgrid with uncertainties based on deep reinforcement learning," *Energy*, vol. 238, p. 121873, 2022, doi: https://doi.org/10.1016/j.energy.2021.121873.

[3] L. Xuan and S. Bin, "Microgrids - An integration of renewable energy technologies," *2008 China Int. Conf. Electr. Distrib. CICED 2008*, 2008, doi: 10.1109/CICED.2008.5211651.

[4] Z. P. Yuan, J. Xia, and P. Li, "Two-Time-Scale Energy Management for Microgrids with Data-Based Day-Ahead Distributionally Robust Chance-Constrained Scheduling," *IEEE Trans. Smart Grid*, vol. 12, no. 6, pp. 4778–4787, Nov. 2021, doi: 10.1109/TSG.2021.3092371.

[5] P. B. S. K. and N. M. P. D. Prudhviraj, "Stochastic Energy Management of Microgrid with Nodal Pricing," *J. Mod. Power Syst. Clean Energy*, vol. 8, no. 1, pp. 102–110, 2020, doi: 10.35833/MPCE.2018.000519.

[6] I. Aghajani, G.R. and Heydari, "Energy management in microgrids containing electric vehicles and renewable energy sources considering demand response," *J. Oper. Autom. Power Eng.*, 2021, doi: 10.22098/joape.2020.5854.1438.

[7] J. P. S. C. A. Rezaee Jordehi, Mohammad Sadegh Javadi, "Energy management in microgrids with battery swap stations and var compensators," *J. Clean. Prod.*, vol. 272, p. 122943, 2020, doi: https://doi.org/10.1016/j.jclepro.2020.122943.

[8] B. E. B. Ssadik Charadi, Houssam Eddine Chakir, Abdelbari Redouane, Abdennebi El Hasnaoui, "A Novel Hybrid Imperialist Competitive Algorithm–Particle Swarm Optimization Metaheuristic Optimization Algorithm for Cost-Effective Energy Management in Multi-Source Residential Microgrids," *Energies*, vol. 16, no. 19, p. 6896, 2023, doi: https://doi.org/10.3390/en16196896.

[9] X.-J. Z. Yan Zhang, Fanlin Meng, Rui Wang, Wanlu Zhu, "A stochastic MPC based approach to integrated energy management in microgrids," *Sustain. Cities Soc.*, vol. 41, pp. 349–362, 2018, doi: https://doi.org/10.1016/j.scs.2018.05.044.

[10] A. I. Fhazhil Wamalwa, "Optimal energy management in a grid-tied solar PV-battery microgrid for a public building under demand response," *Energy Reports*, vol. 12, pp. 3718–3731, 2024, doi: 3718-3731.

[11] J. P. S. C. Seyed Amir Mansouri, Amir Ahmarinejad, Emad Nematbakhsh, Mohammad Sadegh Javadi, Ahmad Rezaee Jordehi, "Energy management in microgrids including smart homes: A multi-objective approach," *Sustain. Cities Soc.*, vol. 69, p. 102852, 2021, doi: https://doi.org/10.1016/j.scs.2021.102852.

[12] S. C. Grace Muriithi, "Optimal Energy Management of a Grid-Tied Solar PV-Battery Microgrid: A Reinforcement Learning Approach," *Energies*, vol. 14, no. 9, p. 2700, 2021, doi: https://doi.org/10.3390/en14092700.

[13] M. P.-C. Daniel Zaldívar, Bernardo Morales, Alma Rodríguez a, Arturo Valdivia-G, Erik Cuevas, "A novel bio-inspired optimization model based on Yellow Saddle Goatfish behavior," *BioSystems*, vol. 174, pp. 1–21, 2018, doi: https://doi.org/10.1016/j.biosystems.2018.09.007.

[14] D. K. J. Angalaeswari S., "Optimal Energy Management Using Sequential Quadratic Programming Algorithm for Stand Alone PV System," *Int. J. Appl. Eng. Res.*, vol. 12, no. 22,

pp. 12250–12255, 2017, [Online]. Available: https://www.ripublication.com/ijaer17/ijaerv12n22_68.pdf
[15] A. I. Fhazhil Wamalwa, "Optimal energy management in a grid-tied solar PV-battery microgrid for a public building under demand response," *Energy Reports*, vol. 12, pp. 3718–3731, 2024, doi: https://doi.org/10.1016/j.egyr.2024.09.054.

s